Chapter 1

Blind Beamforming for IRS without Channel Estimation

After reading this chapter you should be able to:

- Understand the necessity of sidestepping channel estimation for the IRS beamforming in many real-world wireless networks to date.
- Examine the fundamental aspect of the standard method of RMS, i.e., how fast the resulting SNR boost grows with the IRS size and the sample size.
- Understand the rationale behind a statistical blind beamforming method called CSM, and why it guarantees a quadratic SNR boost in the IRS size.
- Interpret the CSM method from a variety of optimization perspectives including the closest point projection and the phase retrieval.

1.1. Introduction

Passive beamforming, i.e., coordinating phase shifts across the reflective elements, lies at the core of the intelligent reflecting surface (IRS) technology. Despite the intrinsic difference between passive beamforming and the conventional active beamforming for the MIMO channels, many existing works on

IRS still follow the traditional model-driven paradigm of first estimating channels and then optimizing phase shifts, thereby readily applying the classical beamforming tools such as semidefinite relaxiation (SDR) [Luo et al., 2010], weighted minimum mean square error (WMMSE) [Shi et al., 2011], and fractional programming (FP) [Shen and Yu, 2018].

However, channel acquisition for an IRS-aided system could pose formidable challenges in engineering practice, mainly in the following three respects:

i. Each reflected channel alone can be easily overwhelmed by the other channels and noise, so it can be difficult to obtain precise estimation.
ii. One has to modify the current networking protocol (e.g., frame structure) to enable channel estimation for IRS. Besides, some channel estimating algorithms entail the full information of the received signal, but this is not supported by many communication chips on the market.
iii. Channel estimation for the reflected channels may incur huge time complexity if the IRS consists of a large number reflective elements.

In order to address the above issues, the past few years have seen a surge of research interests in *blind beamforming* without relying on any channel knowledge. Both [Psomas and Krikidis, 2021] and [Nadeem et al., 2021] advocate a random rotation strategy for passive beamforming in the absence of the instantaneous channel information. Another line of studies [You et al., 2020, Ning et al., 2021, Wang et al., 2022, Wang and Zhang, 2021] suggest simply trying out all possible directions of the reflected beam; this procedure does not require any channel information. However, the above beam sweeping approach is typically restricted to the millimeter/terahertz communication scenario with sharp beams. And deep learning has been considered in this area. As opposed to [Liu et al., 2020, Elbir et al., 2020, Gao et al., 2020, Liu et al., 2021, Huang et al.,

2020, Feng et al., 2020] that use deep learning to either estimate channels or optimize phase shifts given channels, the recent work [Jiang et al., 2021] proposes learning to directly map the received pilot signals to the passive beamforming vector via deep neural networks. It is argued in [Jiang et al., 2021] that such unified learning policy is capable of extracting more pertinent information from the raw data. Differing from these neural net-based approaches, the method called RFocus in [Arun and Balakrishnan, 2020] uses the statistics of the received signal. The present chapter also pursues a statistical approach and shows that the proposed blind beamforming method can strike provable better performance than RFocus in [Arun and Balakrishnan, 2020]. Aside from the theoretical justifications, we further demonstrate this novel blind beamforming method through field tests in a commercial 5G network.

Throughout the chapter, we use the Bachmann-Landau notation extensively: $f(n) = O(g(n))$ if there exists some $c > 0$ such that $|f(n)| \leq cg(n)$ for n sufficiently large; $f(n) = o(g(n))$ if there exists some $c > 0$ such that $|f(n)| < cg(n)$ for n sufficiently large; $f(n) = \Omega(g(n))$ if there exists some $c > 0$ such that $f(n) \geq cg(n)$ for n sufficiently large; $f(n) = \Theta(g(n))$ if $f(n) = O(g(n))$ and $f(n) = \Omega(g(n))$ both hold.

1.2. System Model

For ease of discussion, the majority of the present chapter focuses on the single-user single-antenna transmission; the extension to the general case with multiple users and multiple antennas is postponed till Section 1.5.3. Assume that the IRS consists of a total of N reflective elements. Let $h_n^{\mathrm{I}} \in \mathbb{C}$ be the channel from the transmitter to the nth reflective element, and $h_n^{\mathrm{II}} \in \mathbb{C}$ the channel from

the nth reflective element to the receiver. The cascaded channel h_n associated with the nth reflective element is then obtained as

$$h_n = h_n^{\mathrm{I}} h_n^{\mathrm{II}}, \quad \text{for } n = 1, \ldots, N. \tag{1.1}$$

Let $h_0 \in \mathbb{C}$ be the superposition of the rest channels from the transmitter to the receiver (including the direct channel as well as those reflected channels not due to the IRS). We frequently represent the above channels in a polar form, i.e.,

$$h_n = \beta_n e^{j\alpha_n}, \quad \text{for } n = 0, \ldots, N, \tag{1.2}$$

where the channel magnitude $\beta_n \in (0, 1)$ and the channel phase $\alpha_n \in (0, 2\pi]$. Moreover, use $\theta_n \in (0, 2\pi]$ to denote the phase shift induced by the nth reflective element in its corresponding channel h_n, and $\boldsymbol{\theta}$ the passive beamforming vector $(\theta_1, \ldots, \theta_N)$. Thus, for the transmit signal $X \in \mathbb{C}$, the received signal $Y \in \mathbb{C}$ is given by

$$Y = \left(h_0 + \sum_{n=1}^{N} h_n e^{j\theta_n} \right) X + Z, \tag{1.3}$$

where a complex Gaussian random variable $Z \sim \mathcal{CN}(0, \sigma^2)$ models the additive background noise. Further, for practical reasons, we assume that each θ_n is selected from a prescribed discrete set

$$\Phi_K = \{\omega, 2\omega, \ldots, K\omega\}, \tag{1.4}$$

where K is the number of phase shift choices and the distance ω is given by

$$\omega = \frac{2\pi}{K}. \tag{1.5}$$

For the field tests as shown in Section 1.6, we adopt $K = 4$ and $\omega = \pi/2$, namely the quadrature phase shifting.

Assuming a mean transmit power of P, i.e., $\mathbb{E}[|X|^2] = P$, the signal-to-noise ratio (SNR) can be computed as

$$\mathsf{SNR} = \frac{\mathbb{E}[|Y - Z|^2]}{\mathbb{E}[|Z|^2]} = \frac{P}{\sigma^2} \left| \beta_0 e^{j\alpha_0} + \sum_{n=1}^{N} \beta_n e^{j(\alpha_n + \theta_n)} \right|^2 . \tag{1.6}$$

Notice that we are only interested in how much the SNR could be improved by configuring the IRS properly, rather than the specific value of SNR. Toward this end, we define the baseline case without IRS to be

$$\mathsf{SNR}_0 = \frac{P\beta_0^2}{\sigma^2}, \tag{1.7}$$

and consider the *SNR boost* $f(\boldsymbol{\theta})$ as follows:

$$f(\boldsymbol{\theta}) := \frac{\mathsf{SNR}}{\mathsf{SNR}_0} = \frac{1}{\beta_0^2} \left| \beta_0 e^{j\alpha_0} + \sum_{n=1}^{N} \beta_n e^{j(\alpha_n + \theta_n)} \right|^2 . \tag{1.8}$$

The IRS beamforming task is now formulated as a combinatorial optimization problem of maximizing the SNR boost over the discrete phase shifts:

$$\underset{\boldsymbol{\theta}}{\text{maximize}} \quad f(\boldsymbol{\theta}) \tag{1.9a}$$

$$\text{subject to} \quad \theta_n \in \Phi_K \text{ for } n = 1, \ldots, N. \tag{1.9b}$$

We remark that the channel information $\{h_0, \ldots, h_N\}$ is not available in the above problem setup. A common approach in the literature is to first estimate channels and subsequently optimize $\boldsymbol{\theta}$ explicitly in (1.9). Nevertheless, as elaborated in Section 1.3, channel acquisition can be quite costly in practice. A

blind beamforming approach is then proposed to optimize $\boldsymbol{\theta}$ in the absence of channel information. As the main contribution of this chapter, we illustrate a somewhat surprising result that a statistical blind beamforming method is capable of reaching the global optimum without knowing the channels.

1.3. Random-Max Sampling (RMS)

The simplest method for blind beamforming is just to try out a bunch of random samples of $\boldsymbol{\theta}$ and then choose the best, referred to as the *random-max sampling (RMS)* method. Specifically, we generate a total of T samples of $\boldsymbol{\theta}$ at random. For the tth sample denoted as $\boldsymbol{\theta}_t = (\theta_{1t}, \ldots, \theta_{Nt})$, each entry θ_{nt} is drawn uniformly and independently from the discrete set Φ_K. The received signal corresponding to the tth random sample is given by

$$Y_t = \left(h_0 + \sum_{n=1}^{N} h_n e^{j\theta_{nt}} \right) X_t + Z_t. \tag{1.10}$$

The RMS method simply decides $\boldsymbol{\theta}$ according to the received signal power, i.e.,

$$\boldsymbol{\theta}^{\text{RMS}} = \boldsymbol{\theta}_{t^\star} \ \text{ where } \ t^\star = \arg \max_{1 \le t \le T} |Y_t|^2. \tag{1.11}$$

Clearly, the sample size T plays a key role in the performance of RMS. Before proceeding to the performance analysis, we first define the *average per element reflection power gain* to be

$$\bar{\beta}^2 = \frac{1}{N} \sum_{n=1}^{N} \beta_n^2. \tag{1.12}$$

The following theorem shows how the SNR boost by RMS grows with the sample size T and the IRS size N.

Theorem 1.1: *Consider T i.i.d. random samples of $\boldsymbol{\theta}$ uniformly drawn over Φ_K. The expected SNR boost achieved by the RMS method in* (1.11) *has the following order bounds:*

$$\mathbb{E}\big[f(\boldsymbol{\theta}^{RMS})\big] = \frac{\bar{\beta}^2}{\beta_0^2} \cdot \Theta(N \log T) \;\; \textit{if} \;\; T = o(\sqrt{N}), \tag{1.13}$$

$$\mathbb{E}\big[f(\boldsymbol{\theta}^{RMS})\big] = \frac{\bar{\beta}^2}{\beta_0^2} \cdot O(N \log T) \;\; \textit{in general}, \tag{1.14}$$

where the expectation is taken over random samples of $\boldsymbol{\theta}$.

The proof of the above theorem is beyond the scope of this chapter. We refer the interested readers to [Ren et al., 2021] for the mathematical details.

But how far is this scaling rate of RMS from the optimum? To answer this question, we construct an upper bound on the SNR boost by assuming that the channels are already known and also that each phase shift θ_n can be arbitrarily chosen on $(0, 2\pi]$. It can be easily seen that under the above two assumptions the maximum SNR boost is achieved when every phase-shifted reflected channel $h_n e^{j\theta_n}$ is aligned with the direct channel h_0 exactly. In other words, each θ_n is optimally determined as

$$\theta_n = \alpha_0 - \alpha_n. \tag{1.15}$$

Plugging the above θ_n into (1.8) yields an upper bound on the achievable SNR boost as stated in the following theorem.

Theorem 1.2: *The SNR boost is bounded from above as*

$$f(\boldsymbol{\theta}) \leq \frac{\left(\sum_{n=0}^{N} \beta_n\right)^2}{\beta_0^2}, \tag{1.16}$$

and thus it is at most quadratic in the number of reflective elements, i.e.,

$$f(\boldsymbol{\theta}) = \frac{\bar{\beta}^2}{\beta_0^2} \cdot O(N^2). \tag{1.17}$$

Consequently, the highest SNR boost we can expect for RMS (and also for any other algorithms) is quadratic in N. According to Theorem 1.1, it takes an exponential number of samples for RMS to reach this upper bound, i.e., $T = \Omega(2^N)$. Intuitively, RMS can figure out the optimal $\boldsymbol{\theta}$ only after it has almost exhausted the entire solution space of Φ_K^N. But is it possible to figure out the optimal solution by using merely a polynomial number of samples? The next section aims to answer the above question.

1.4. Conditional Sample Mean (CSM)

In this section we propose a novel statistical method that is guaranteed to achieve the quadratic SNR boost much more efficiently than RMS. We still generate T random samples of $\boldsymbol{\theta}$ in a uniform and independent fashion, only that T just needs to be polynomially large as shown in the end of this section.

We begin by defining $\mathcal{Q}_{nk} \subseteq \{1, \ldots, T\}$ to be the subset of the indices of all those random samples with $\theta_{nt} = k\omega$, i.e.,

$$\mathcal{Q}_{nk} = \{t : \theta_{nt} = k\omega\}, \;\; \forall n = 1, \ldots, N \text{ and } \forall k = 1, \ldots, K. \tag{1.18}$$

Algorithm 1 Conditional Sample Mean (CSM)

input: Φ_K, N, T;
for $t = 1, 2, \ldots, T$ **do**
  generate $\boldsymbol{\theta}_t = (\theta_{1t}, \ldots, \theta_{Nt})$ i.i.d. based on Φ_k;
  measure received signal power $|Y_t|^2$ with $\boldsymbol{\theta}_t$;
end for
for $n = 1, 2, \ldots, N$ **do**
  for $k = 1, 2, \ldots, K$ **do**
    compute $\widehat{\mathbb{E}}[|Y|^2 | \theta_n = k\omega]$ according to (1.19);
  end for
  decide θ_n^{CSM} according to (1.20);
end for
output: $\boldsymbol{\theta}^{\mathrm{CSM}} = (\theta_1^{\mathrm{CSM}}, \ldots, \theta_N^{\mathrm{CSM}})$.

A conditional sample mean of the received signal power $|Y|^2$ is computed within each subset $\mathcal{Q}_{nk}$, denoted by

$$\widehat{\mathbb{E}}[|Y|^2 \,|\, \theta_n = k\omega] = \frac{1}{|\mathcal{Q}_{nk}|} \sum_{t \in \mathcal{Q}_{nk}} |Y_t|^2. \tag{1.19}$$

The main idea of the *conditional sample mean (CSM)* method is to choose each θ_n such that the corresponding conditional sample mean is maximized:

$$\theta_n^{\mathrm{CSM}} = \arg\max_{\varphi \in \Phi_K} \widehat{\mathbb{E}}[|Y|^2 \,|\, \theta_n = \varphi]. \tag{1.20}$$

The above method is summarized in Algorithm 1.

The intuition behind CSM follows. We use $\widehat{\mathbb{E}}[|Y|^2 | \theta_n = k\omega]$ to measure the average goodness of a particular choice $\theta_n = k\omega$ when the rest θ_m's are still pending. With all the phase shifts determined in this way simultaneously, a kind of equilibrium among the N reflective elements can be reached. We examine this equilibrium in the following theorem.

Theorem 1.3: *Consider T i.i.d. random samples of $\boldsymbol{\theta}$ uniformly drawn over*

Φ_K. *When $K \geq 3$, the expected SNR boost achieved by the CSM method in Algorithm 1 has a tight order bound:*

$$\mathbb{E}[f(\boldsymbol{\theta}^{CSM})] = \frac{\bar{\beta}^2}{\beta_0^2} \cdot \Theta(N^2) \ \ \textit{if} \ T = \Omega(N^2(\log N)^3), \tag{1.21}$$

where the expectation is taken over random samples of $\boldsymbol{\theta}$.

Two observations in the above scaling law analysis of CSM are worth noting. First, CSM requires only a polynomial number of random samples to attain the quadratic SNR boost in N, which makes CSM much more practical than the standard method of RMS. Second, the quadratic scaling rate of CSM holds only when $K \geq 3$; we will delve into this issue in Section 1.5.1.

1.5. Some Comments on CSM

1.5.1. Connection to Closest Point Projection

In Section 1.3 we assume that the channel information is already known and also that each phase shift can be arbitrarily chosen on $(0, 2\pi]$ as $K \to \infty$, in order to derive an upper bound on the SNR boost. The resulting optimal θ_n is shown in (1.15). What if we only make the first assumption (i.e., channel information available) whereas the number of phase shift choices K is still finite?

A simple method under the above new setting is to project the relaxed continuous solution, which is given in (1.15), to the closest point within the discrete set Φ_K, referred to as the *closest point projection (CPP)* method. If the projection is performed in the Euclidean distance sense, then each θ_n is

determined as

$$\theta_n^{\mathrm{CPP}} = \arg\min_{\varphi \in \Phi_K} \left|\varphi - \alpha_0 + \alpha_n\right|. \tag{1.22}$$

CPP can be alternatively interpreted as choosing each θ_n such that $h_n e^{j\theta_n}$ is rotated to the closest possible position to h_0 on the complex plane. We are interested in this CPP method because of its close connection to CSM, as specified in the following theorem.

Theorem 1.4: *The CSM method without channel information is equivalent to the CPP method with channel information if the sample size is sufficiently large, i.e.,*

$$\boldsymbol{\theta}^{CSM} = \boldsymbol{\theta}^{CPP} \ \ \textit{as } n \to \infty. \tag{1.23}$$

Proof. When the phase shift of the nth reflective element is fixed at $k\omega$, the received signal is given by

$$Y = \left(h_0 + h_n e^{jk\omega}\right) X + \left(\sum_{m=1, m\neq n}^{N} h_m e^{j\theta_m}\right) X + Z. \tag{1.24}$$

Furthermore, assuming that the rest phase shifts are randomly and independently chosen from the discrete set Φ_K, and also that X is i.i.d. with $\mathbb{E}[|X|^2] = P$ and Z is drawn i.i.d. from $\mathcal{CN}(0, \sigma^2)$, the conditional expectation of the received signal power can be computed as

$$\begin{aligned}
\mathbb{E}\left[|Y|^2 \,|\, \theta_n = k\omega\right] &= \mathbb{E}_{\theta_m, X, Z} \left| \left(h_0 + h_n e^{jk\omega}\right) X + \left(\sum_{m=1, m\neq n}^{N} h_m e^{j\theta_m}\right) X + Z \right|^2 \\
&= \left|h_0 + h_n e^{jk\omega}\right|^2 P + \sum_{m=1, m\neq n}^{N} \beta_m^2 P + \sigma^2 \\
&= 2\beta_0 \beta_n P \cos(k\omega - \alpha_0 + \alpha_n) + \sum_{m=0}^{N} \beta_m^2 P + \sigma^2. \qquad (1.25)
\end{aligned}$$

By the law of large numbers, the conditional sample mean $\widehat{\mathbb{E}}[|Y|^2 \,|\, \theta_n = k\omega]$ in (1.19) approaches the above value when the sample size increases. Consequently, as $T \to \infty$, the CSM method in (1.20) boils down to

$$\theta^{\text{CSM}} = \arg \max_{\theta_n \in \Phi_K} \mathbb{E}\left[|Y|^2 \,|\, \theta_n = k\omega\right] \tag{1.26}$$

$$= \arg \max_{\theta_n \in \Phi_K} \cos(\theta_n - \alpha_0 + \alpha_n). \tag{1.27}$$

Clearly, the solution of (1.27) is to make θ_n close to $\alpha_0 - \alpha_n$ as much as possible, namely the CPP method. The equivalence between CPP and CSM as $T \to \infty$ is thus established.

We further show that CPP yields a constant approximation ratio factor for any fixed K.

Theorem 1.5: *The CPP method in* (1.22) *satisfies*

$$\cos^2(\pi/K) \cdot f^\star \leq f(\boldsymbol{\theta}^{CPP}) \leq f^\star, \tag{1.28}$$

where $f^\star$ is the maximum SNR boost.

Proof. The right inequality is evident. We focus on showing the left inequality in what follows:

$$f(\boldsymbol{\theta}^{\text{CPP}}) = \frac{1}{\beta_0^2} \cdot \left| \beta_0 e^{j\alpha_0} + \sum_{n=1}^{N} \beta_n e^{j\left(\theta_n^{\text{CPP}} + \alpha_n\right)} \right|^2 \tag{1.29a}$$

$$= \frac{1}{\beta_0^2} \cdot \left| \beta_0 + \sum_{n=1}^{N} \beta_n e^{j\left(\theta_n^{\text{CPP}} - \alpha_0 + \alpha_n\right)} \right|^2 \tag{1.29b}$$

$$\geq \frac{1}{\beta_0^2} \cdot \left| \beta_0 + \sum_{n=1}^{N} \beta_n \cos\left(\theta_n^{\text{CPP}} - \alpha_0 + \alpha_n\right) \right|^2 \tag{1.29c}$$

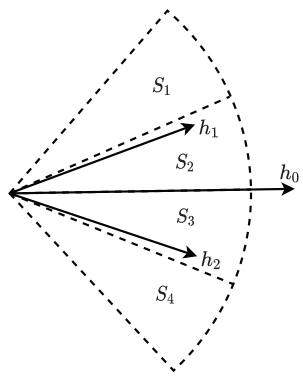

Figure 1.1: Consider four sectors $\{\mathcal{S}_1, \mathcal{S}_2, \mathcal{S}_3, \mathcal{S}_4\}$; each sector spans an angle of π/K. For $N = 2$, assume that h_0 is located right between $\mathcal{S}_2$ and $\mathcal{S}_3$, and that h_1 is inside $\mathcal{S}_2$ but arbitrarily close to $\mathcal{S}_1$, while h_2 and h_1 are symmetric about h_0. When $K = 4$ and $|h_1| = |h_2|$, it follows that h_1 and h_2 cancel out each other under CPP or CSM, so IRS does not boost SNR.

$$\geq \frac{1}{\beta_0^2} \cdot \left(\beta_0 + \sum_{n=1}^{N} \beta_n \cos(\pi/K) \right)^2 \tag{1.29d}$$

$$\geq \frac{\cos^2(\omega/2)}{\beta_0^2} \cdot \left(\sum_{n=0}^{N} \beta_n \right)^2 \tag{1.29e}$$

$$\geq \cos^2(\omega/2) \cdot f^\star, \tag{1.29f}$$

where (1.29c) follows since each $\beta_n e^{j(\theta_n^{\mathrm{CPP}} - \alpha_0 + \alpha_n)} = \beta_n \cos(\theta_n^{\mathrm{CPP}} - \alpha_0 + \alpha_n) + j\beta_n \sin(\theta_n^{\mathrm{CPP}} - \alpha_0 + \alpha_n)$ and the removal of the sin component does not decrease the absolute square, (1.29d) follows by the fact that $|\theta_n^{\mathrm{CPP}} - \alpha_0 + \alpha_n| \leq \pi/K$ under the closest point projection, and (1.29f) follows by the upper bound in Theorem 1.2. The proof is then completed.

Incorporating the above result into Theorem 1.4 partly verifies the scaling law of CSM in Theorem 1.3, as stated in the following corollary.

Corollary 1.1: *For CPP, the approximation ratio* $\cos^2(\pi/K) \geq 0.5$ *if* $K \geq 3$,

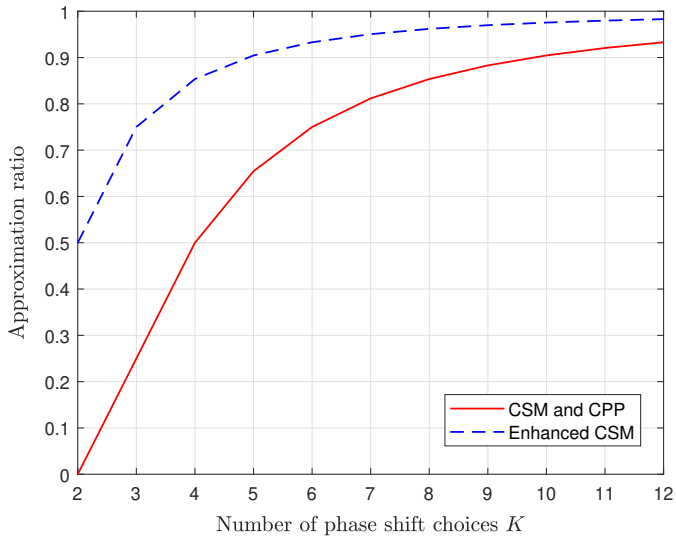

Figure 1.2: Consider four sectors $\{\mathcal{S}_1, \mathcal{S}_2, \mathcal{S}_3, \mathcal{S}_4\}$; each sector spans an angle of π/K. For $N = 2$, assume that h_0 is located right between $\mathcal{S}_2$ and $\mathcal{S}_3$, and that h_1 is inside $\mathcal{S}_2$ but arbitrarily close to $\mathcal{S}_1$, while h_2 and h_1 are symmetric about h_0. When $K = 4$ and $|h_1| = |h_2|$, it follows that h_1 and h_2 cancel out each other under CPP or CSM, so IRS does not boost SNR.

whereas $\cos^2(\pi/K) = 0$ *if* $K = 2$. *Consequently, as* $T \to \infty$, *CSM optimally reaches a quadratic SNR boost in* N *if* $K \geq 3$, *whereas its SNR boost cannot be bounded from below if* $K = 2$.

Fig. 1.1 gives a concrete example to illustrate the failure of CSM when $K = 2$. Notice that the above corollary only claims that CSM would be equivalent to CPP when the sample size T is sufficiently large. It entails considerable efforts to verify the specific threshold on T as stated in Theorem 1.3; the interested readers are referred to [Ren et al., 2021] for the complete proof of Theorem 1.3.

Furthermore, an enhanced CSM can yield a quadratic SNR boost in the

number of reflective elements N for any $K \geq 2$. The main idea is to improve the approximation ratio factor of CPP, as shown in Fig. 1.2. Observe that the enhanced CSM yields an approximation ratio factor of 0.5 even at $K = 2$, so it guarantees a quadratic SNR boost for the binary beamforming case. More details can be found in [Ren et al., 2021].

1.5.2. Connection to Phase Retrieval

Although CSM does not perform channel estimation explicitly, we can somehow retrieve the phase information of the channels $\{h_0, h_1, \ldots, h_N\}$ from the beamforming decision $\boldsymbol{\theta}$ by CSM.

When all the θ_n's are uniformly and independently distributed over Φ_K, the expectation of the received signal power is given by

$$\mathbb{E}[|Y|^2] = \beta_0^2 P + \sum_{m=1}^{N} \beta_m^2 P + \sigma^2. \tag{1.30}$$

When a particular θ_n is fixed at $k\omega$ and the rest θ_m's are randomized, the resulting conditional expectation of the received signal power is given by

$$\mathbb{E}\big[|Y|^2 \,|\, \theta_n = k\omega\big] = P\big|h_0 + h_n e^{jk\omega}\big|^2 + \sum_{m \neq n} \beta_m^2 P + \sigma^2. \tag{1.31}$$

We use J_{nk} to denote the difference between the above two expectations, which can be computed as

$$J_{nk} = \mathbb{E}[|Y|^2 \,|\, \theta_n = k\omega] - \mathbb{E}[|Y|^2] \tag{1.32a}$$

$$= 2\beta_0\beta_n P \cos(k\omega - \alpha_0 + \alpha_n). \tag{1.32b}$$

Observe that the value of J_{nk} depends on the phase difference

$$\Delta_n = \alpha_0 - \alpha_n \tag{1.33}$$

between the direct channel h_0 and the reflected channel h_n.

Moreover, the above expectation difference can be evaluated empirically based on the random samples, i.e.,

$$\widehat{J}_{nk} = \frac{1}{|\mathcal{Q}_{nk}|} \sum_{t \in \mathcal{Q}_{nk}} |Y_t|^2 - \frac{1}{T} \sum_{t=1}^{T} |Y_t|^2. \tag{1.34}$$

The main idea of phase retrieval is to recover the phase difference Δ_n through minimizing the gap between J_{nk} and $\widehat{J}_{nk}$. For instance, if we consider a *square-max* loss function

$$\mathcal{L}_n(\Delta_n) = \left| \max_{1 \le k \le K} \left\{ J_{nk} \right\} - \max_{1 \le k \le K} \left\{ \widehat{J}_{nk} \right\} \right|^2, \tag{1.35}$$

then the phase retrieval problem is formulated as

$$\underset{\{\Delta_n\}}{\text{minimize}} \quad \sum_{n=1}^{N} \mathcal{L}_n(\Delta_n) \tag{1.36a}$$

$$\text{subject to} \quad 0 \le \Delta_n < 2\pi, \quad \text{for } n = 1, \ldots, N. \tag{1.36b}$$

The above problem can be optimally solved as

$$\Delta_n = k_0 \omega \ \text{ where } \ k_0 = \arg \max_{1 \le k \le K} \widehat{\mathbb{E}}[|Y|^2 \,|\, \theta_n = k\omega]. \tag{1.37}$$

An analogy can be immediately seen between the above solution and the CSM method in (1.20), both of which seek the phase shift $\theta_n \in \Phi_K$ to maximize the

conditional sample mean $\widehat{\mathbb{E}}[|Y|^2 \mid \theta_n = k\omega]$. Thus, CSM boils down to recovering the phase difference Δ_n according to the loss function in (1.35).

But we could have used a different loss function in the phase retrieval. If $\mathcal{L}_n(\Delta_n)$ in problem (1.36) is replaced with the following *sum-of-squares* loss function

$$\mathcal{L}'_n(\Delta_n) = \sum_{k=1}^{K} \left| J_{nk} - \widehat{J}_{nk} \right|^2, \tag{1.38}$$

the solution of Δ_n becomes

$$\Delta_n = \begin{cases} -\arctan \dfrac{F_n}{E_n} + \dfrac{\pi}{2} & \text{if } E_n \geq 0, \\ -\arctan \dfrac{F_n}{E_n} - \dfrac{\pi}{2} & \text{if } E_n < 0, \end{cases} \tag{1.39}$$

where

$$E_n = \sum_{k=1}^{K} \widehat{J}_{nk} \sin(k\omega) \quad \text{and} \quad F_n = \sum_{k=1}^{K} \widehat{J}_{nk} \cos(k\omega). \tag{1.40}$$

If the closest point projection is performed based on the above Δ_n, i.e., $\theta_n = \arg\min_{\varphi \in \Phi_K} |\varphi - \Delta_n|$, we would arrive at another version of CSM. Furthermore, it turns out that every choice of loss function in the phase retrieval problem (1.36) can be recognized as a variation of the CSM method.

1.5.3. CSM for General Utility Functions

The CSM method can be further extended to a general utility function in order to account for multiple users and multiple antennas. For each random sample $t = 1, \ldots, T$, we now measure a utility value $U_t \in \mathbb{R}$ at the receiver side. For instance, if we have multiple users and aim at a max-min fairness, the utility could be set to the minimum SNR among the users.

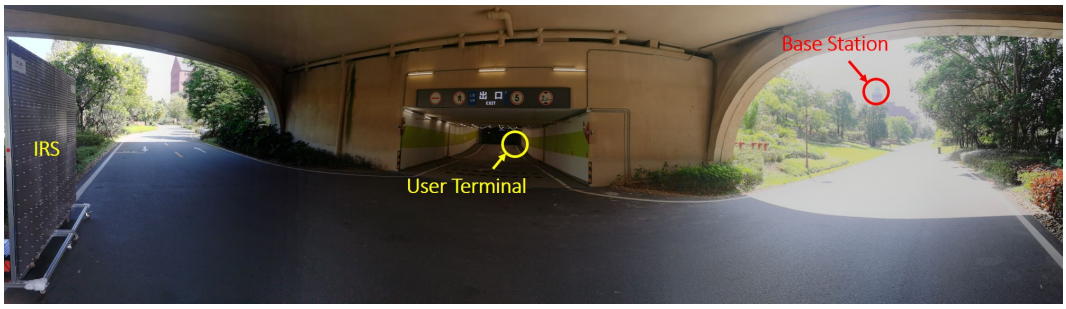

Figure 1.3: A panoramic view of the field test site. The base station is located on a 20-meter-high terrace while the user terminal is located inside an underground parking lot. The IRS is placed at the entrance of the parking lot. The IRS is approximately 250 meters away from the base station, and the user terminals are approximately 40 meters away from the IRS.

Recall the conditional sample subset $\mathcal{Q}_{nk}$ in (1.18). We now compute the conditional sample mean of U within each subset $\mathcal{Q}_{nk}$, i.e.,

$$\widehat{\mathbb{E}}[U \mid \theta_n = k\omega] = \frac{1}{|\mathcal{Q}_{nk}|} \sum_{t \in \mathcal{Q}_{nk}} U_t. \tag{1.41}$$

Following Algorithm 1, we decide each θ_n according to the respective conditional sample mean, i.e.,

$$\theta_n^{\mathrm{CSM}} = \arg\max_{\varphi \in \Phi_K} \widehat{\mathbb{E}}[U \mid \theta_n = \varphi]. \tag{1.42}$$

Deciding the optimal utility function for the generalized CSM remains an open problem.

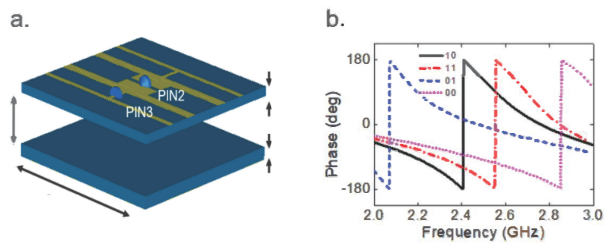

Figure 1.4: The ON-OFF state of a PIN diode results in two distinct resonance frequencies in the series RLC circuit, which correspond to two phase shifts. Further, with a pair of PIN diodes integrated into each reflective element, we can realize four phase shifts by controlling the respective ON-OFF states of the two PIN diodes.

1.6. Field Tests

In this section we demonstrate the performance of the blind beamforming approach through prototype tests in the real-world wireless environment. Our tests are carried out in a public downlink network over a 200 MHz wide spectrum band centered at 2.6 GHz. It is worth pointing out that our blind beamforming method does not require any collaboration from the service provider side. Thus, the IRS can be deployed and then configured in a plug-and-play fashion.

The hardware realization of each reflective element is illustrated in Fig. 1.4. A quadrature beamforming with $\theta_n \in \{0, \pi/2, \pi, 3\pi/2\}$ is implemented by using a pair of PIN diodes at each reflective element. Moreover, as shown in Fig. 1.5, the IRS is formed by 16 "reflecting tiles"—a tiny IRS prototype that is $50\,\text{cm} \times 50\,\text{cm}$ large—arranged in a 4×4 array. Each reflecting tile consists of 16 reflective elements, so the assembled large IRS consists of 256 reflective elements in total. There are 4 phase shift choices $\{0, \pi/2, \pi, 3\pi/2\}$ for each individual reflective element.

As shown in Fig. 1.3 and Fig. 1.6, the base station is located on a 20-meter-

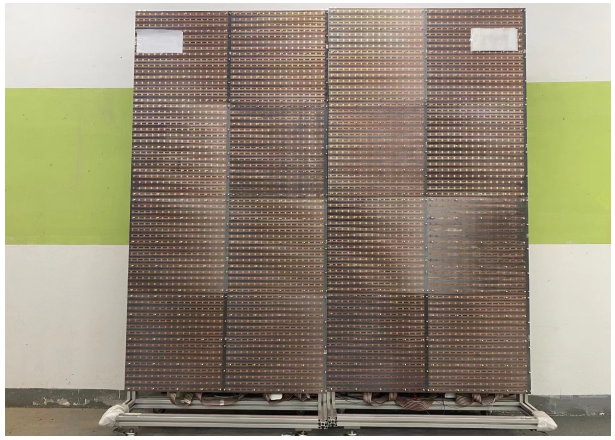

Figure 1.5: The IRS is formed by a 4×4 array of reflecting tiles. Each reflecting tile is 50cm×50cm large and consists of 16 reflective elements.

Table 1.1: Performance of the different algorithms

Algorithm	SISO RSRP boost (dB)	SISO SINR boost (dB)	MIMO SE increment (bps/Hz)
CSM	4.02	3.57	2.02
RMS	-3.93	-3.84	1.97
OFF	-1.69	-1.69	0.77

high terrace while the user terminal is located in an underground parking lot. There is no line-of-sight propagation from the base station to the user terminal. The IRS is placed outdoors near the entrance of the parking lot. The distance from the base station to the IRS is approximately 250 meters; the distance from the IRS to the user terminal is approximately 40 meters. It is worth remarking that the wireless environment is highly volatile in our case because of the busy traffic in the parking lot, as can be observed from Fig. 1.7.

We use the sample size $T = 2560$ (i.e., $T = 10N$) for both RMS and CSM. Moreover, we include a baseline method called "OFF", which simply fixes the phase shift θ_n at the initial state without beamforming.

We start with the single-input single-output (SISO) transmission, aiming

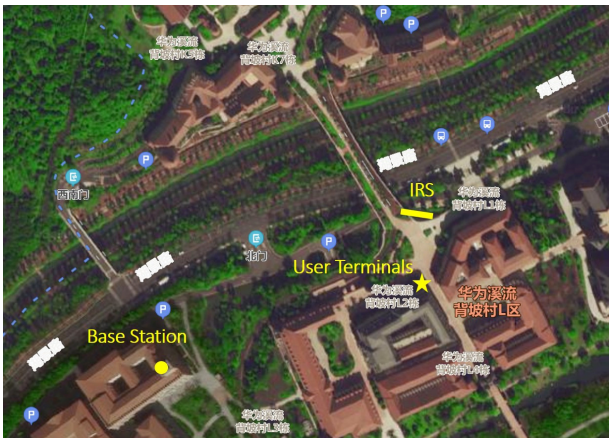

Figure 1.6: A satellite image of the field test site. The base station and the IRS are outdoor while the user terminals are indoor.

to improve the SNR boost. There are two measurements: Reference Signal Received Power (RSRP) and Signal-to-Interference-plus-Noise Ratio (SINR). Notice that the SNR cannot be measured directly because of co-channel interference. Following the definition of the SNR boost, we let the RSRP (or SINR) boost be the ratio between the achieved RSRP (or SINR) and the baseline RSRP (or SINR) without IRS. Fig. 1.9 shows the RSRP boosts achieved by the various methods. It can be seen that CSM outperforms the other methods significantly. CSM gives an approximately 5 dB improvement upon CSM and OFF. As shown in the figure, although CSM encounters two sharp drops, which are due to the shadowing effect caused by vehicles, its overall performance is still more consistent over time than RMS and OFF. Observe from Fig. 1.9 that the RSRP boost by OFF is mostly below 0 dB; the reason is that the reflected signals without proper beamforming can result in a destructive superposition. Observe also that RMS yields the worst RSRP performance, even 4 dB lower than not using IRS. This surprising result indicates that, in a complicated wireless environment with interference and noise, the beamformer

Figure 1.7: The view from the user terminal toward the IRS.

decision based on the best single sample is not reliable.

We further compare the SINR boosts of the various methods in Fig. 1.8. It can be seen that the SINR boosts and the RSRP boosts have similar profiles. The average RSRP boosts and the average SINR boosts are summarized in Table 1.1. According to the table, the SINR gain is smaller than the RSRP gain. One reason for this gain reduction is that IRS incurs additional reflected interference. Nevertheless, the constructive effect on the desired signals outweighs that on the interfering signals. As a result, CSM can still bring considerable performance gains as compared to the benchmark methods and not using CSI.

Moreover, we consider the MIMO transmission. In our case, the base station has 64 transmit antennas while the user terminal has 4 receive antennas, so at most 4 data streams are supported. Because the base station is a black box to us, how the transmit precoding is performed is unknown. We use the generalized CSM in Section 1.5.3 and let the utility be the *Spectral Efficiency (SE)*. Thus, we measure the SE in bps/Hz at the user terminal for each random sample. Fig. 1.10 shows the SE increments by the various algorithms against

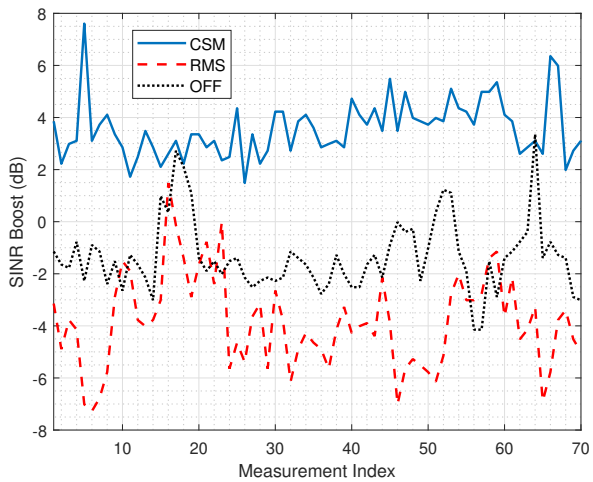

Figure 1.8: SINR boost for SISO transmission.

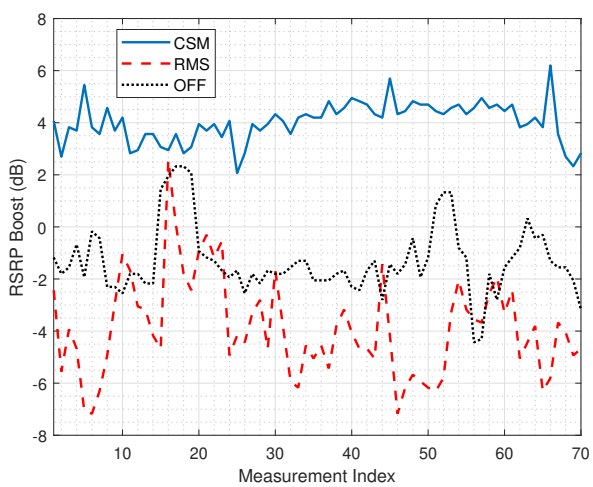

Figure 1.9: RSRP boost for SISO transmission.

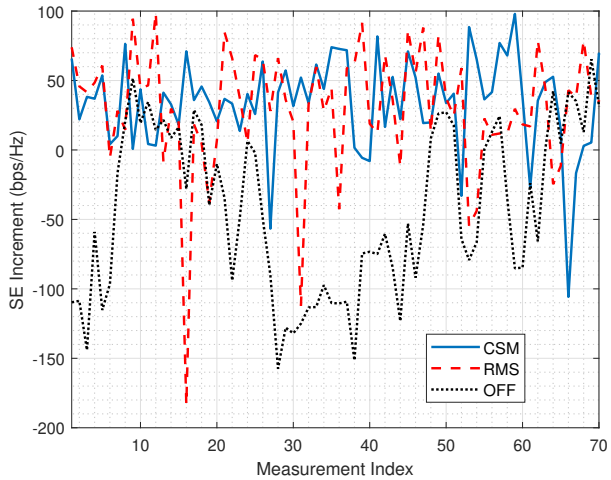

Figure 1.10: SE increment for MIMO transmission.

the baseline SE without IRS. Observe that all the algorithms can bring improvements, although OFF occasionally gives negative effects. The figure shows that RMS becomes more robust in the MIMO case. Actually, RMS is sometimes even better than CSM, but it still has inferior performance on average. The average SE increment results summarized in Table 1.1 agree with what we observe from Fig. 1.10.

1.7. Conclusion

In this chapter we consider passive beamforming for IRS without any channel information, because channel acquisition can be costly and technically difficult in practice. We begin with the standard method of RMS—which simply tries out different beamformer samples at random and chooses the best, but it requires an exponentially large number of samples to achieve a quadratic SNR boost in the number of reflective elements. In contrast, the proposed statistical

blind beamforming method called CSM is capable of achieving the quadratic SNR boost by using merely a polynomial number of samples. We then examine CSM from the closest point projection and the phase retrieval points of view. Furthermore, CSM can be enhanced to reach a higher approximation ratio and can be extended to the multi-user multi-antenna scenario by means of utility function. Finally, we demonstrate the effectiveness of CSM in improving the data transmission in a commercial 5G network.

Bibliography

V. Arun and H. Balakrishnan. RFocus: Beamforming using thousands of passive antennas. In *USENIX Symp. Netw. Sys. Design Implementation (NSDI)*, pages 1047–1061, February 2020.

A. M. Elbir, A. Papazafeiropoulos, P. Kourtessis, and S. Chatzinotas. Deep channel learning for large intelligent surfaces aided mm-Wave massive MIMO systems. *IEEE Wireless Commun. Lett.*, 9(9):1447–1451, September 2020.

K. Feng, Q. Wang, X. Li, and C.-K. Wen. Deep reinforcement learning based intelligent reflecting surface optimization for MISO communication systems. *IEEE Wireless Commun. Lett.*, 9(5):745–749, May 2020.

J. Gao, C. Zhong, X. Chen, H. Lin, and Z. Zhang. Unsupervised learning for passive beamforming. *IEEE Commun. Lett.*, 24(5):1052–1056, May 2020.

C. Huang, R. Mo, and C. Yuen. Reconfigurable intelligent surface assisted multiuser MISO systems exploiting deep reinforcement learning. *IEEE J. Sel. Areas Commun.*, 38(8):1839–1850, August 2020.

T. Jiang, H. V. Cheng, and W. Yu. Learning to reflect and to beamform for intelligent reflecting surface with implicit channel estimation. *IEEE J. Sel. Areas Commun.*, 39(6):1913–1945, July 2021.

C. Liu, X. Liu, D. W. K. Ng, and J. Yuan. Deep residual network empowered channel estimation for IRS-assisted multi-user communication systems. In *IEEE Int. Commun. Conf.*, June 2021.

S. Liu, Z. Gao, J. Zhang, M. D. Renzo, and M.-S. Alouini. Deep denoising neural network assisted compressive channel estimation for mmWave intelligent reflecting surfaces. *IEEE Trans. Veh. Technol.*, 69(8):9223–9228, August 2020.

Z.-Q. Luo, W.-K. Ma, A. M. So, Y. Ye, and S. Zhang. Semidefinite relaxation of quadratic optimization problems. *IEEE Mag. Signal Process.*, 27(3):20–34, May 2010.

Q.-U.-A. Nadeem, A. Zappone, and A. Chaaban. Intelligent reflecting surface enabled random rotations scheme for the MISO broadcast channel. *IEEE Trans. Wireless Commun.*, 20(8):5226–5242, March 2021.

B. Ning, Z. Chen, W. Chen, Y. Du, and J. Fang. Terahertz multi-user massive MIMO with intelligent reflecting surface: Beam training and hybrid beamforming. *IEEE Trans. Veh. Technol.*, 70(2):1376–1393, February 2021.

C. Psomas and I. Krikidis. Low-complexity random rotation-based schemes for intelligent reflecting surfaces. *IEEE Trans. Wireless Commun.*, 20(8): 5212–5225, March 2021.

S. Ren, K. Shen, Y. Zhang, X. Li, X. Chen, and Z.-Q. Luo. Configuring intelligent reflecting surface with perfor-

mance guarantees: Blind beamforming. [Online]. Available https://kaimingshen.github.io/doc/BlindBeamforming.pdf, 2021.

K. Shen and W. Yu. Fractional programming for communication systems—Part I: Power control and beamforming. *IEEE Trans. Signal Process.*, 66 (10):2616–2630, May 2018.

Q. Shi, M. Razaviyayn, Z.-Q. Luo, and C. He. An iteratively weighted mmse approach to distributed sum-utility maximization for a mimo interfering broadcast channel. *IEEE Trans. Signal Process.*, 59(9):4331–4340, September 2011.

P. Wang, J. Fang, W. Zhang, and H. Li. Fast beam training and alignment for IRS-assisted millimeter wave/Terahertz systems. *IEEE Trans. Wireless Commun.*, 21(4):2710–2724, April 2022.

W. Wang and W. Zhang. Joint beam training and positioning for intelligent reflecting surface assisted millimeter wave communications. *IEEE Trans. Commun.*, 20(10):6282–6297, October 2021.

C. You, B. Zheng, and R. Zhang. Fast beam training for IRS-assisted multi-user communications. *IEEE Wireless Commun. Lett.*, (11):1845–1849, November 2020.